Chaotic proton dynamics in the hydrogen bond

R. Grauer, K. H. Spatschek, and A. V. Zolotaryuk*
Institut für Theoretische Physik I, Heinrich-Heine-Universität Düsseldorf, D-4000 Düsseldorf, Germany
(Received 4 December 1991; revised manuscript received 22 May 1992)

The motion of a proton in a double-well potential created by the potentials of two heavy ions in a molecular chain is considered. The topology of the potential changes depending on the distance between the molecules. Both forms, double well and single well, are possible. Individual chaotic proton motion is triggered by the oscillations of the lattice. Depending on the system parameters, both the one-well and the cross-well attractors can be either periodic or chaotic. This has some interesting consequences for the interpretation and understanding of propagation of ionic defects in hydrogen-bonded chains in the presence of external oscillating fields. A frequency-locked propagating kink is found.

PACS number(s): 05.45.+b, 03.40.Kf, 05.60.+w, 87.22.Fy

I. INTRODUCTION

The transport of energy and charge along one-dimensional chains of hydrogen bonds is an extremely important problem in bioenergetic and solid-state situations. The molecular systems that we study in the present paper are long periodic chains of hydrogen bonds forming channels for the proton transport. The proton transfer is carried out along the hydrogen bonds between various sidegroups having, e.g., hydroxyl, carboxyl, amino, or amide groups and also tightly bound water molecules which can be involved in the chain. One-dimensional chains of hydrogen bonds also exist in alcohols, carbohydrates, imidazole, etc. Here, we do not care too much about the details of the chain but concentrate on one general aspect: Protonic conductivity of such systems in the direction of the hydrogen-bonded chains in about 10^3 times greater than in the perpendicular directions.

In the past the proton motion in a molecular chain was investigated by many authors with many interesting results. (For a comprehensive review see, for example, Ref. [1].) Most of the authors emphasized the collective aspect when calculating the intrabond proton transfer associated with ionic-defect propagation. They found that the structure and dynamics of the ionic defects in hydrogen-bonded one-dimensional systems can be of soliton type [2–5]. A one-component model leads to stable propagating kink or antikink solutions for the proton displacements. These solutions, when interpreted from the physical point of view, describe very well-ordered motions of the protons in the external potentials. In one-component models, each proton interacts with its neighbors (e.g., through harmonic forces) and moves in an externally imposed on-site potential which has (at least) two minima with equal energy and can be thought of as arising from a rigid-background lattice.

Already at the early stages of those theories it was correctly argued that the one-component models have to be generalized by taking into account a soft-background lattice through the motion of the surrounding heavy ions, vibrations of the sublattices, etc. Then, e.g., within a two-component model, the interaction between the relative displacements of protons and heavy ions was taken into account, and again (now two-component) solitary-wave solutions were found and discussed [3,6–10]. The second component introduces also a feature that has not been considered so far. In contrast to the rigid-background approximation, oscillations of the sublattice can occur, and besides the usual (stationary) two-component solitary-wave solutions, time-dependent (triggered) collective motions might also be possible. The investigation of such driven solitary waves is extremely important since the ubiquitous damping will stop the propagation of (quasistationary) two-component solitary waves and lead to an extinction of that type of collective transport. Thus we should also look for other types of collective transport. However, when taking into account a driven proton motion, we should be aware of a possible destruction of ordered transport due to chaos. The investigation of that aspect is the main intent of the present paper. Let us elucidate the idea by starting from models representing the present state of the art in nonlinear theory of proton motion in the hydrogen bond.

Up until now, various groups worked on generalizations of two-component models. For example, a two-sublattice model for the ionic defects in hydrogen-bonded chains was recently considered in [10] and [11]. It contains many aspects of previous models and starts from the Hamiltonian

$$H = l^2 m \sum_n \left\{ \frac{1}{2} \left[\frac{dq_n}{dt} \right]^2 + \frac{1}{2} \frac{c_0^2}{l^2} (q_{n+1} - q_n)^2 + \frac{1}{ml^2} U(q_n, Q_n, Q_{n+1}) \right\} + l^2 M \sum_n \left\{ \frac{1}{2} \left[\frac{dQ_n}{dt} \right]^2 + \frac{1}{2} \frac{v_0^2}{l^2} (Q_{n+1} - Q_n)^2 + \frac{1}{Ml^2} V_i(Q_n) \right\} . \quad (1.1)$$

This model describes a diatomic chain with two masses m

and M, where m is the proton mass and M is the mass of the heavy ion. Furthermore, $q_n = y_n/l$ is the dimensionless displacement of the proton in the nth hydrogen bridge from the middle of the nth and $(n+1)$th heavy ions, under the assumption that the latter are in their equilibrium positions. The $Q_n = Y_n/l$ are the dimensionless displacements of the heavy ions from their equilibrium positions, and l is the lattice spacing for both sublattices. The velocities c_0 and v_0 result from the cooperative nature of the hydrogen bonding and correspond to the acoustic modes in the light and heavy sublattices, respectively. The potential $U(q_n, Q_n, Q_{n+1})$ is an on-site proton potential originating, e.g., from the Morse potentials of the heavy ions. Therefore, it also depends on the distances $Q_{n+1} - Q_n$ in the heavy-ion sublattice and moves together with the ions. The potential $V_i(Q_n)$ is a single-well substrate potential for the heavy-ion sublattice which takes into account the environment of the hydrogen-bonded chain.

The canonical equations following from the Hamiltonian (1.1) are

$$\frac{d^2 q_n}{dt^2} = \frac{c_0^2}{l^2}(q_{n+1} - 2q_n + q_{n-1}) - \frac{1}{ml^2}\frac{\partial}{\partial q_n} U(q_n, Q_n, Q_{n+1}) , \tag{1.2}$$

$$\frac{d^2 Q_n}{dt^2} = \frac{v_0^2}{l^2}(Q_{n+1} - 2Q_n + Q_{n-1}) - \frac{1}{Ml^2}\frac{\partial}{\partial Q_n}\left[V_i(Q_n) + \sum_m U(q_m, Q_m, Q_{m+1}) \right] . \tag{1.3}$$

Introducing the new coordinates

$$u_n = q_n - R_n , \tag{1.4}$$

$$R_n = \tfrac{1}{2}(Q_n + Q_{n+1}) , \tag{1.5}$$

$$\rho_n = Q_{n+1} - Q_n , \tag{1.6}$$

we can rewrite (1.2) and (1.3) as

$$\frac{d^2 u_n}{dt^2} = \frac{c_0^2}{l^2}(u_{n+1} - 2u_n + u_{n-1}) + \omega_i^2 R_n + \frac{1}{2}\frac{c_0^2}{l^2}(1 - s_0^2)(\rho_{n+1} - \rho_{n-1}) - \left[1 + \frac{\mu}{2}\right]\frac{1}{ml^2} f_n - \frac{\mu}{2}\frac{1}{ml^2}[\tfrac{1}{2}(f_{n-1} + f_{n+1}) + g_{n+1} - g_{n-1}] , \tag{1.7}$$

$$\frac{d^2 R_n}{dt^2} = \frac{v_0^2}{l^2}(R_{n+1} - 2R_n + R_{n-1}) - \omega_i^2 R_n + \frac{\mu}{2}\frac{1}{ml^2}[\tfrac{1}{2}(f_{n-1} + f_{n+1}) + f_n + g_{n+1} - g_{n-1}] , \tag{1.8}$$

$$\frac{d^2 \rho_n}{dt^2} = \frac{v_0^2}{l^2}(\rho_{n+1} - 2\rho_n + \rho_{n-1}) - \omega_i^2 \rho_n + \frac{\mu}{ml^2}[\tfrac{1}{2}(f_{n+1} - f_{n-1}) + g_{n+1} - 2g_n + g_{n-1}] . \tag{1.9}$$

Here, we assumed V_i to be a quadratic potential and have introduced the notations

$$\omega_i^2 = \frac{1}{Ml^2}\frac{\partial^2 V_i}{\partial Q_n^2}\bigg|_{Q_n = 0} ,$$

$$f_n = \frac{\partial U(u_n, \rho_n)}{\partial u_n} , \tag{1.10}$$

$$g_n = \frac{\partial U(u_n, \rho_n)}{\partial \rho_n} ,$$

$$\mu = \frac{m}{M} , \quad s_0 = v_0/c_0 . \tag{1.11}$$

At this stage, three directions for proceeding are possible. In the first (traditional) one, the possible (stationary) solitary-wave solutions of (1.7)–(1.9) are analyzed. We shall come back to this point, and the corresponding open problems, in the final part of the paper. Here, we want to start with the second approach, i.e., the individual point of view for the motion. This will enable us to appreciate the third direction, i.e., the time-dependent collective one, with novel aspects of solitary-wave transport by time-dependent solutions.

For the *individual* point of view let us simplify Eqs. (1.7)–(1.9) by neglecting the dispersive contributions (by formally setting $v_0 = c_0 = 0$) and ignoring higher-order terms in the mass ratio μ. Then we obtain

$$\frac{d^2 u_n}{dt^2} \approx \omega_i^2 R_n - \frac{1}{ml^2}\frac{\partial U(u_n, \rho_n)}{\partial u_n} , \tag{1.12}$$

$$\frac{d^2 \rho_n}{dt^2} \approx -\omega_i^2 \rho_n , \tag{1.13}$$

$$\frac{d^2 R_n}{dt^2} \approx -\omega_i^2 R_n , \tag{1.14}$$

i.e., the motion of the proton in the potential U and under the influence of (external) oscillations of the heavy-ion sublattice. In the following we shall, for the purpose of simplicity, neglect the effects due to the motion of the mass centers R_n (by setting $R_n = 0$). Then the two coupled equations (1.12) and (1.13) remain to be solved. From this individual point of view, each proton is decoupled from the others but moves under the influence of the nonlinear potential U. Due to the huge inertia of the heavy-ion sublattice, we can assume that the oscillations in ρ_n (and, for the more general case, the R_n oscillations

also) persist for a long time and act like an external driver in (1.12).

This situation reminds us very strongly of the Duffing oscillator [when the obvious damping of the proton motion is also included in (1.12)]. Although our actual problem is different from the Duffing oscillator, one can expect that here also interesting and perhaps exotic effects due to the nonlinear dynamics occur. (We should remind the reader that even for the Duffing oscillator not all phenomena are understood. An excellent review of the present state of the art can be found, e.g., in a most recent paper by Ueda *et al.* [12].) Here we shall concentrate on two aspects of the individual proton motion in the on-site potential of heavy ions: (i) the intersection of stable and unstable manifolds for the present oscillator problem with topological changes in the potential caused by heavy sublattice oscillations and (ii) the proton escape from a potential well and the jump from one-well to cross-well motions. We expect that the one-well and cross-well attractors can be either periodic or chaotic, and we want to determine the parameter values for the various regions. This is important since the problem of stable (collective) solitary-wave motion in the region of chaotic individual motion has, to our knowledge, so far been neither attacked nor solved.

To study in a nontraditional manner the *collective* proton dynamics in the basic equations of motion (1.7)–(1.9) we assume $c_0 \neq 0$ and simplify them as follows. As in the case of the individual proton motion, we neglect the effects due to the inertia of the heavy ions (by putting formally $\mu=0$). Therefore, the latter may be considered as external drivers. We further assume that at any instant of time the heavy ions move opposite to each other with the same speeds. In other words, we take into account only the optical mode of the heavy-ion sublattice. In this case, it is obvious that the mass centers are immobile, i.e., $R_n=0$ and $\rho_{n-1}=\rho_{n+1}$. Thus, Eq. (1.12) is transformed into

$$\frac{d^2u_n}{dt^2} \approx \frac{c_0^2}{l^2}(u_{n+1}-2u_n+u_{n+1}) - \frac{1}{ml^2}\frac{\partial}{\partial u_n}U(u_n,\rho_n) \; . \tag{1.15}$$

The ρ_n oscillations will be considered as external drivers. We shall then investigate whether a frequency-locked kink propagation is possible.

In this paper we consider both the dissipative case of a periodically parameter-forced second-order Morse oscillator (individual proton motion) and the stationary as well as nonstationary soliton models (for collective proton motion). We want to find out whether, similar to the individual results, a resonant collective motion also exists. The manuscript is organized as follows: In Sec. II the individual aspects are investigated. First, the equations of motion of a proton in a parameter-dependent double-well potential are formulated. Then the equations are solved numerically. The numerical findings are compared with analytical estimates by Melnikov theory. In Sec. III the collective aspects are considered by discussing simplified soliton models and their solutions. A frequency-locked kink mode is detected. The paper is concluded by a short summary and outlook.

II. INDIVIDUAL PROTON DYNAMICS

A. Equation of motion

Let us consider two molecules (or heavy ions) where the equilibrium distance between them is denoted by l. Each of these molecules creates a pair potential $V(r)$ for some light ion (say, proton) of the topology shown in Fig. 1. In the following we use r as the distance parameter. In an isolated molecule the potential minimum is at r_0. Consider now two neighboring molecules (heavy ions) of the same type. Superimposing the two potentials $V(r)$ created by the two molecules, we obtain a double potential $U(r)$. When the heavy ions are in their equilibrium positions (or close to them), the two ion-proton potentials form a double-well potential for the common proton. This scenario is motivated by the well-known phenomena in hydrogen-bonded chains. Here, we take into account that the heavy ions are in general not stationary. They may be oscillating or forced to move close to each other, and at some critical distance the topology of the total potential $U(r)$ might change, e.g., from the double-well potential to a potential with a single minimum. It is clear that the double-well potential $U(r)$ depends on the relative displacement of the heavy ions. Let us assume the following notations (see Fig. 2). The variable ρ denotes the deviation of the distance of the heavy ions from the equilibrium value; u is the dimensionless (all lengths are in units of l which is the equilibrium distance between two heavy ions in the lattice) displacement of the proton from the middle between the heavy ions; and the equilibrium positions $\pm u_0$ depend on the relative displacement ρ, and $u_0(\rho=0)$ is denoted by q_0.

If the function $V(r)$ is given for $0<r<\infty$, the function $U(u,\rho)$ can be constructed as the following sum:

$$U(u,\rho)=V\left[\frac{1+\rho}{2}+u\right]+V\left[\frac{1+\rho}{2}-u\right] - V(\tfrac{1}{2}+q_0)-V(\tfrac{1}{2}-q_0) \; . \tag{2.1}$$

Then the equilibrium distances $u_0=u_0(\rho)$ will be found as the nontrivial roots of the equation

$$V'((1+\rho)/2+u_0)=V'((1+\rho)/2-u_0) \; ,$$

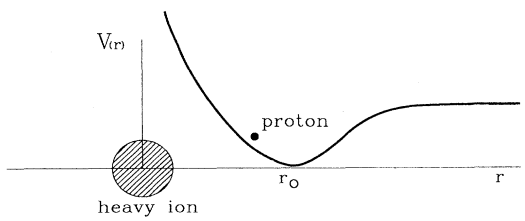

FIG. 1. Potential of a molecule (heavy ion) as a function of distance. The potential has a single minimum where a proton can find its equilibrium position.

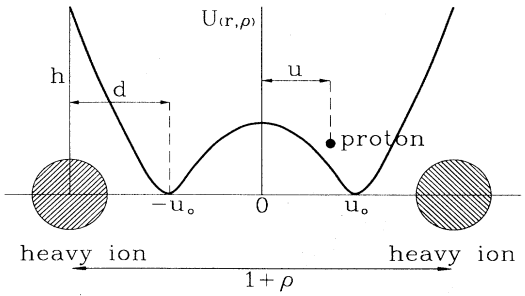

FIG. 2. Notations for a double-well potential created from the two Morse potentials.

where the prime denotes the derivative with respect to the argument. In principle, the function $V(r)$, $0<r<\infty$, may be any of the standard potentials (Morse, Lennard-Jones, etc.), but the situation can be generalized to include any symmetric function $U(u,\rho)$ with a correct physical behavior in both the variables u and ρ. For demonstration, we shall present in the following analytic and numerical calculations for the case of two Morse potentials. Each one of them is of the form

$$V(r)=D_0[1-e^{-b(r-r_0)}]^2 , \tag{2.2}$$

with positive constants D_0 (dissociation energy) and b (potential parameter). In this case, a straightforward calculation leads to

$$U(u,\rho)=\frac{D_0}{\alpha^2}\{[\alpha-\cosh(bu)e^{-b\rho/2}]^2+\tfrac{1}{2}(1-e^{-b\rho})\} , \tag{2.3}$$

where

$$\alpha=\cosh(bq_0)=\tfrac{1}{2}\exp[b(\tfrac{1}{2}-r_0)] .$$

For $\rho\equiv 0$, the function (2.3) has two minima only if the parameter b satisfies the inequality

$$b>\frac{\ln 2}{\frac{1}{2}-r_0} , \quad r_0<\tfrac{1}{2} . \tag{2.4}$$

In a general case, when $\rho\neq 0$, the positions of the minima $\pm u_0$ also can be found analytically.

At

$$\rho_c=2(\ln 2/b+r_0)-1<0 ,$$

the double-well potential is transformed to the single-well form. For $\rho<\rho_c$, the potential remains of single-well form.

In order to be close to the well-known Duffing oscillator, we can introduce the potential (normalized to be of the harmonic form for small u when $\rho\equiv 0$)

$$\bar{U}(u,\rho)=\frac{\alpha^2}{D_0}\frac{1}{2b^2(\alpha-1)}\left[U-\frac{D_0}{\alpha^2}(\alpha-1)^2\right] . \tag{2.5}$$

For $1<\alpha<4$ the potential (2.5) has the double-well form. For the realistic parameter values, α indeed lies in this interval.

Introducing

$$\tau=(\alpha+1)^{-1/2}\omega_0 t\equiv\bar{\omega}t, \quad \omega_0^2\equiv\frac{2D_0b^2(\alpha^2-1)}{\alpha^2 ml^2} , \tag{2.6}$$

we find the equation of motion

$$\frac{d^2u}{d\tau^2}+\frac{\partial}{\partial u}\bar{U}(u,\rho)=0 . \tag{2.7}$$

Equation (2.7) is in suitable form for mathematical considerations. For applications we take $D_0=5.11$ eV (water molecule dissociation $H_2O\rightarrow OH^-+H^+$), $l=2.76$ Å, $r_0 l=0.96$ Å,

$$b=(2.64\ \text{Å}^{-1})l=7.298 ,$$

leading to $\alpha=1.518$ and $\bar{\omega}=622.4$ THz. Here we have used the proton mass

$$m=1.6726\times 10^{-27}\ \text{kg} .$$

The oscillations of the heavy ions we assume to be harmonic, i.e., of the form

$$\rho(\tau)=\rho_0\sin(\Omega\tau) . \tag{2.8}$$

In general, a damping term for the proton also has to be included in (2.7). Therefore, we may generalize (2.7) to

$$\frac{d^2u}{d\tau^2}+\frac{\partial}{\partial u}\bar{U}(u,\rho)=-\gamma\frac{du}{d\tau} . \tag{2.9}$$

In the *adiabatic limit* the proton moves much more rapidly than the heavy ions (for $\gamma=0$). Therefore, in this limit for any instant of time the displacement ρ may be considered to be strictly constant. Then Eq. (2.7) [with $\rho\equiv$const] can be integrated by using standard techniques. But the *nearly adiabatic case* with $\rho\neq$const and $\gamma>0$ seems to be more interesting and realistic. In this latter case we investigate whether we can have stochastic behavior of the proton if the amplitude ρ_0 exceeds a critical value $|\rho_{\text{crit}}|$. To attack this problem, we solve numerically Eq. (2.9) with $\rho=\rho_0\sin(\Omega\tau)$. Here, e.g., $\gamma=0.1$ is used for a damping on the τ time scale, and the dimensionless frequency Ω for the heavy-ion oscillations follows from the following considerations: The positions of the heavy ions (relative to their equilibrium positions) are only in the simplest approximation described by (2.8). In general, the motion of the heavy ions is influenced (despite the hydrogen bond) by a harmonic bonding (leading to acoustic modes) and the substrate potential V_i (leading to optical modes). Then the motion of the heavy ions follows from the Hamiltonian

$$H_i=l^2M\sum_n\left[\frac{1}{2}\left[\frac{dQ_n}{dt}\right]^2+\frac{1}{2}\left[\frac{v_0}{l}\right]^2(Q_{n+1}-Q_n)^2+\frac{1}{Ml^2}V_i(Q_n)\right] . \tag{2.10}$$

This part of the Hamiltonian has been already presented in Sec. I. The substrate potential leads to a characteristic (linear) frequency ω_i. As has been discussed in the Introduction, the approximation (2.8) follows from (2.10) when dispersion and nonlinear effects are neglected. In the nearly adiabatic limit, $\omega_i\ll\bar{\omega}$ holds because of $m\ll M$,

and therefore as a typical value for Ω, we shall use $\Omega=0.25$ in (2.8).

B. Numerical results

With the help of numerical simulations, we want to answer two questions: (1) Does chaotic motion exist and (2) when does the dynamics on the attractor allow cross-well motion? To tackle the first question, we first investigate numerically the crossing of the stable and unstable manifolds of the hyperbolic periodic orbit $(u,u_t)=(0,0)$. We start with 1000 points very close to the unstable orbit on the unstable (stable) manifold and integrate forward (backward) in time. The results are shown in Figs. 3(a)–3(c) corresponding to situations before, at, and after the tangent crossing. In the Hamiltonian case a transversal crossing would be sufficient to produce chaotic motion, whereas in the dissipative case this need not be true. In this case, as in the Duffing equation, there exists a long, very complicated transient until it finally settles

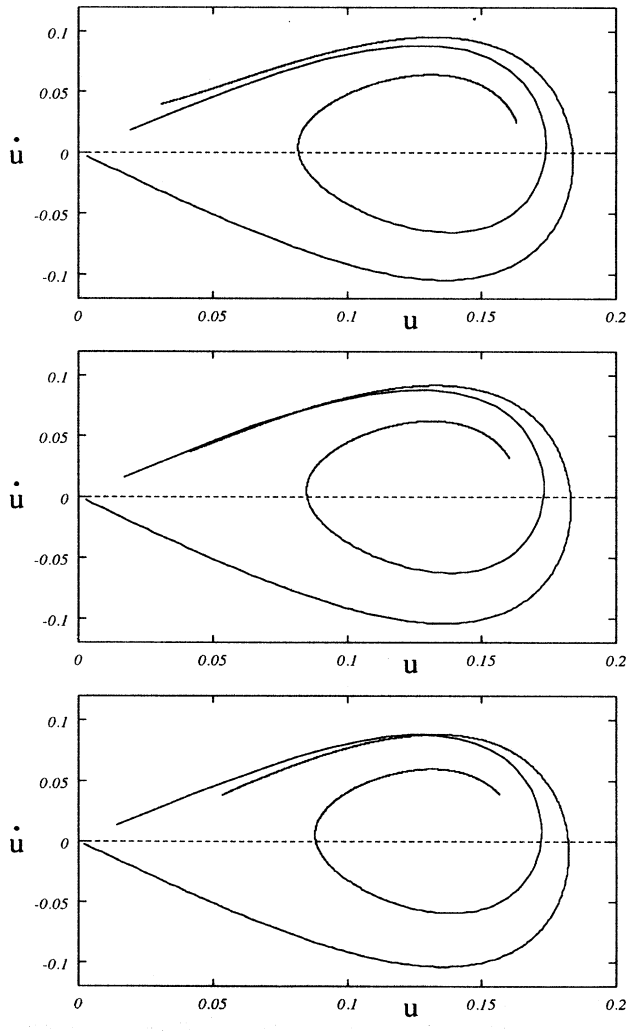

FIG. 3. Crossing of the stable and unstable manifolds for $\rho_0=0.03$, 0.035, 0.04 (from top to bottom, respectively) for fixed $\alpha=1.518$, $b=7.298$, $\gamma=0.1$, and $\Omega=0.25$.

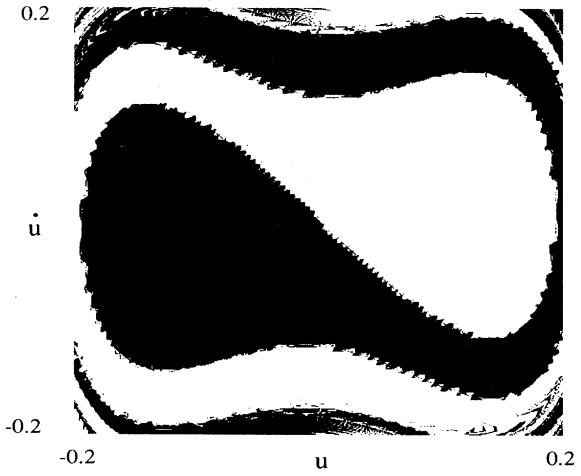

FIG. 4. Basin of attraction (dark for the left) of the stable periodic orbit after the tangent crossing of the stable and unstable manifolds: $\rho_0=0.04$. The other parameter values are the same as in Fig. 3.

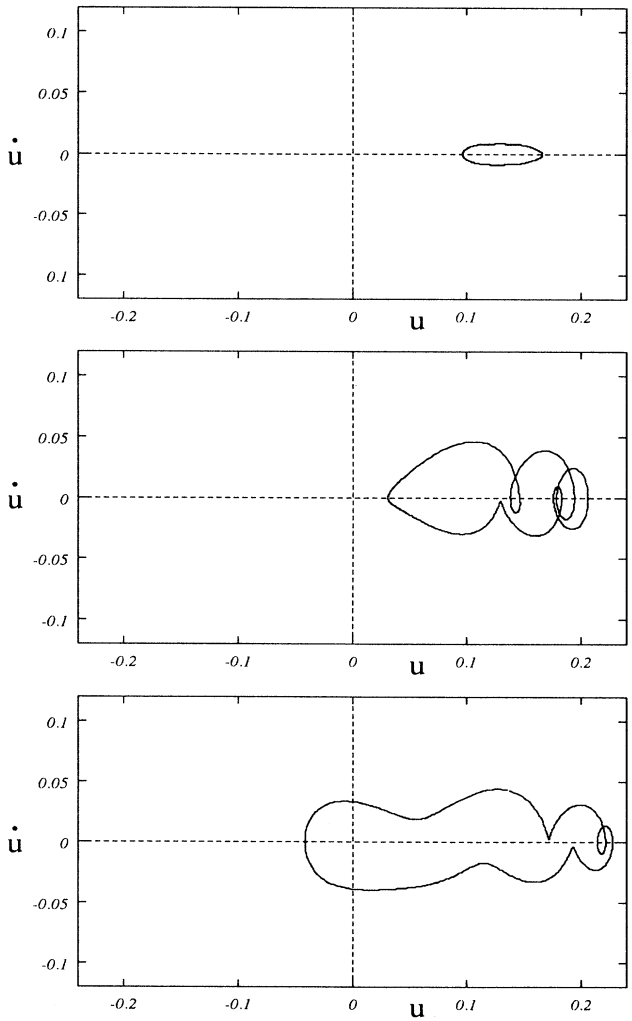

FIG. 5. Periodic orbits for $\rho_0=0.05$, 0.1, 0.15 (from top to bottom, respectively). The other parameters are the same as in Fig. 3.

down to one of the stable periodic orbits. One can demonstrate this by looking at the basin of attraction of the stable periodic orbit (Fig. 4) after the tangent crossing. The picture shows only little deviations from the undriven problem. Crossing of stable and unstable manifolds gives only the criterion for the onset of chaotic motion in the limit of low dissipation when the transient times are much longer than the time scale of the propagation.

To answer finally the question of when chaotic motion starts to exist, we integrate the ordinary differential equation (2.9) for a bunch of initial conditions, varying the driving amplitude ρ_0 and keeping the damping γ fixed. The procedure is a combination of the "Varosi" interpolation [13] with cell-mapping techniques [14], as extensively done in [15]. This method allows us to effectively calculate attractors and their basins. An overview of the results is presented in Table I. As one can easily see, the critical values of the driving ρ_0 are independent of the damping γ. The critical values are roughly given by the criterion that the double-well potential changes (at a certain time) to a single-well potential. Those values are given by $\rho_0=(2/b)\ln\alpha$, $\rho_0=0.11$ for $\alpha=1.518$, and $\rho_0=0.059$ for $\alpha=1.25$, whereas the numerically obtained values are $\rho_0\approx 0.10$ and $\rho_0\approx 0.05$, respectively.

Figures 5(a)–5(c) depict the stable periodic orbits (continuously in time) for various values of the driving. Figures 5(a) and 5(b) show how the orbits approach the center of the potential well as the driving increases. When the driving is big enough such that the orbit can cross the center of the potential well, chaotic motion can start to exist. Looking again at Table I, one observes that for $\alpha=1.518$ and $\rho_0=0.15$, a stable periodic orbit exists independent of the damping. This orbit is shown in Fig. 5(c). All these findings have interesting consequences for the collective motion, as will be discussed in Sec. III.

C. Analytical estimates

Some of the numerical findings can be understood analytically by Melnikov theory. Using (2.5), we write the total Hamiltonian as

$$\bar{H}=\frac{1}{2}\left[\frac{du}{d\tau}\right]^2+\bar{U}\ . \tag{2.11}$$

We treat the ρ oscillations as perturbations and expand

$$\bar{U}(u,\rho)\approx\bar{U}(u,\rho=0)+\frac{\rho}{2b(\alpha-1)}\{\tfrac{1}{2}+\cosh(bu)[\alpha-\cosh(bu)]\}\ . \tag{2.12}$$

Using the representation $(u,v=\dot{u})$, we obtain from (2.11) and (2.12)

$$\dot{v}\equiv\frac{dv}{d\tau}\approx-\left.\frac{\partial\bar{U}}{\partial u}\right|_{\rho=0}-\frac{\rho}{2(\alpha-1)}\{\sinh(bu)[\alpha-2\cosh(bu)]\}\ , \tag{2.13}$$

and the equation of motion can be written as

$$\dot{u}=v\ , \tag{2.14}$$

TABLE I. Attractors for various values of ρ_0, γ, and α. The values of Ω and b are fixed to 0.25 and 7.298, respectively. P1,P2, ... correspond to periodic orbits of periods 1,2, ..., "single" denotes that the proton is observed only in one potential well at the stroboscopic times, LR ... means that the proton jumps from the left to the right potential well and vice versa, and "cross chaotic" means that the chaotic attractor connects the left and right halves of the potential well.

ρ_0	$\alpha=1.518$ $\gamma=0.1$	$\alpha=1.518$ $\gamma=0.05$	$\alpha=1.518$ $\gamma=0.01$	$\alpha=1.518$ $\gamma=0.001$	$\alpha=1.25$ $\gamma=0.1$
0.01	P1 single	P1 single	P1 single	P1 single	P1 single
0.02	P1 single	P1 single	P1 single	P1 single	P1 single
0.03	P1 single	P1 single	P1 single	P1 single	P1 single
0.04	P1 single	P1 single	P1 single	P1 single	P1 single
0.05	P1 single	P1 single	P1 single	P1 single	Cross chaotic
0.06	P1 single	P1 single	P1 single	P1 single	P2, LR, ...
0.07	P1 single	P1 single	P1 single	P1 single	P2, LR, ...
0.08	P1 single	P1 single	P1 single	P1 single	P1 single
0.09	P1 single	P1 single	P1 single	P1, P3 single	P1 single
0.10	P1 single	P1 single	P1 single	P1, P3 single	Cross chaotic
0.11	Chaotic, LR, ...	Chaotic, LR, ...	Cross chaotic	Cross chaotic	P2, LR, ...
0.12	P2, LR, ...	Chaotic, LR, ...	Cross chaotic	Cross chaotic	P2, LR, ...
0.13	Cross chaotic	Chaotic, LR, ...	Cross chaotic	P4, LR	P1 single
0.14	P2 single	High period LR, ...	Cross chaotic	Cross chaotic	P1 single
0.15	P1 single	P1 single	P1 single	P1 single	Cross chaotic
0.16	Chaotic single	Cross chaotic	Cross chaotic	Cross chaotic	
0.17	Cross chaotic	Cross chaotic	Cross chaotic	Chaotic single	
0.18	P2, LR, ...	P2, LR, ...	Cross chaotic		
0.19	P2, LR, ...	Cross chaotic	Cross chaotic		
0.20	P2, LR, ...	Cross chaotic	Cross chaotic		

$$\dot{v}=-\left.\frac{\partial \bar{U}}{\partial u}\right|_{\rho=0}+\tilde{g} \ , \tag{2.15}$$

where the perturbation $\tilde{g}$ follows from (2.9) and (2.13) as

$$\tilde{g}=-\gamma\dot{u}-\frac{\rho_0}{2(\alpha-1)}\{\sinh(bu)[\alpha-2\cosh(bu)]\}\times\sin(\Omega\tau) \ . \tag{2.16}$$

Next we calculate the homoclinic orbit for the undisturbed system ($\gamma=0$, $\rho=0$, $g\equiv 0$) described by the Hamiltonian (2.11) for $\rho\equiv 0$. It is given by the integral

$$\int_{u_0^+}^{u}\frac{du}{\{(\alpha-1)^2-[\alpha-\cosh(bu)]^2\}^{1/2}}=-\frac{1}{b\sqrt{\alpha-1}}\tau \ , \tag{2.17}$$

for $0\le u\le u_0^+$, where u_0^+ is the solution of

$$e^{bu_0^{\pm}}\equiv z_0^{\pm}=\pm 2\alpha\left[1-\frac{1}{\alpha}\right]^{1/2}-(1-2\alpha) \ . \tag{2.18}$$

Introducing the variable $z\equiv\exp(bu)$, we can rewrite (2.17) as

$$I(z)-I(z_0^+)\equiv\int_{z_0^+}^{z}\frac{dz}{(z-1)\{-\frac{1}{4}+(\alpha-\frac{1}{2})z-\frac{1}{4}z^2\}^{1/2}}=-\frac{\tau}{\sqrt{\alpha-1}} \ . \tag{2.19}$$

The integral can be performed analytically to yield

$$I(z)=\frac{2}{A}\ln\frac{-A+2B+(\alpha-1)\dfrac{C(z)}{B+D(z)}}{A+2B+(\alpha-1)\dfrac{C(z)}{B+D(z)}} \ , \tag{2.20}$$

where $A=2\sqrt{\alpha-1}$, $B=\sqrt{\alpha(\alpha-1)}$, $C(z)=1-2\alpha+z$, and

$$D(z)=[-\tfrac{1}{4}+(\alpha-\tfrac{1}{2})z-\tfrac{1}{4}z^2]^{1/2} \ .$$

Using (2.20), we can now determine the homoclinic orbit $u=u^{(0)}$ as a function of τ. Then, of course, $v^{(0)}=\dot{u}^{(0)}$ is also known. It is not necessary to give the explicit expressions for evaluating the Melnikov integral

$$M(\tau_0)\equiv\int_{-\infty}^{+\infty}v^{(0)}\left\{\frac{\rho_0}{2(\alpha-1)}\sinh(bu^{(0)})\times[2\cosh(bu^{(0)})-\alpha]\times\sin(\Omega\tau)\cos(\Omega\tau_0)-\gamma v^{(0)}\right\}d\tau \ . \tag{2.21}$$

On the right-hand side of (2.21), the two integrals

$$I_1\equiv\int_0^{\infty}[v^{(0)}]^2d\tau \tag{2.22}$$

and

$$I_2\equiv\frac{1}{2(\alpha-1)}\int_0^{\infty}v^{(0)}\sinh(bu^{(0)})\times[2\cosh(bu^{(0)})-\alpha]\sin(\Omega\tau)d\tau \tag{2.23}$$

need to be evaluated. A straightforward analysis leads to

$$I_1=-\frac{2}{Ab^2}\int_{z_0^+}^{1}\frac{dz}{\left[\dfrac{d}{dz}I(z)\right]z^2} \tag{2.24}$$

and

$$I_2=-\frac{1}{4b(\alpha-1)}\int_1^{z_0^+}\left[z-\alpha+\frac{\alpha}{z^2}-\frac{1}{z^3}\right]\times\sin\left\{\frac{A\Omega}{2}[I(z_0^+)-I(z)]\right\}dz \ . \tag{2.25}$$

An intersection of the unstable and stable manifolds is predicted by the Melnikov function provided

$$\frac{\rho_0}{\gamma}\ge\left|\frac{I_1}{I_2}\right| \ . \tag{2.26}$$

If we insert the parameter values $\alpha=1.518$, $b=7.298$ (leading to $z_0^+=3.8095$), and $\Omega=0.25$, we obtain from (2.26)

$$\frac{\rho_0}{\gamma}\ge 0.350\,835 \ . \tag{2.27}$$

This agrees excellently with the result of the numerical calculation of the crossing of the stable and unstable manifolds as shown in Figs. 3(a)–3(c). However, when compared to Table I, we recognize that the Melnikov value underestimates the chaos threshold by a fairly large factor. As has been mentioned already, chaos sets in when the double-well potential changes (at a certain time) to a single-well potential.

III. COLLECTIVE PROTON DYNAMICS

A. Stationary solitary-wave solutions

As has been mentioned already in the Introduction, the individual motion of the proton in the potential created by oscillating heavy ions is only one aspect of the whole variety contained in the general model (1.7)–(1.9). Now we briefly mention the other aspect: the existence of stationary (two-component) solitary-wave solutions. These solutions can be obtained either analytically, by using some approximations as described below, or numerically, by using a steepest-descent minimization scheme [11]. In this subsection we review the wide and stationary solitary-wave solutions which can be obtained by standard techniques.

Since the discrete problem is in general difficult to solve and allows only numerical evaluations, we apply the continuum approximation. Introducing the variable $T=c_0t/l$ and the notations $\Omega_0=\omega_0 l/c_0$, $\Omega_i=\omega_i l/c_0$, $f=\partial U/\partial u$, $g=\partial U/\partial\rho$, we obtain, in the case of the potential $V_i(Q_n)=Ml^2\omega_i^2Q_n^2/2$, the coupled set of nonlinear

partial differential equations [10,11]

$$\partial_T^2 u-\partial_x^2 u-\Omega_i^2 R+(s_0^2-1)\rho_x+\Omega_0^2(1+\mu)f+\Omega_0^2\mu g_x=0\ , \tag{3.1}$$

$$\partial_T^2 R-s_0^2\partial_x^2 R+\Omega_i^2 R-\Omega_i^2\mu(f+g_x)=0\ , \tag{3.2}$$

$$\partial_T^2\rho-s_0^2\partial_x^2\rho+\Omega_i^2\rho-\Omega_0^2\mu f_x=0\ , \tag{3.3}$$

where the subscript $x=n$ on f and g denotes a derivative with respect to x. By definition, the stationary solutions depend on x and T through the variable $\xi=x-sT$. Equations (3.1)–(3.3) admit two-component (stationary) solitary-wave solutions in some regions of the velocity s within the interval $0\le s\le 1$.

The two-component models are significant generalizations of the one-component ansatz. In the latter, one neglects any dynamical influence of the heavy sublattice on the proton motion. The position of the proton evolves in this simple case ($\Omega_i=\mu=\rho=0$) according to

$$\partial_T^2 u-\partial_x^2 u+\Omega_0^2 f=0\ . \tag{3.4}$$

Let us discuss the case of two Morse potentials,

$$f=\frac{\partial}{\partial u}\left[\frac{1}{2b^2(\alpha^2-1)}(\alpha-\cosh(bu))^2\right]$$
$$=\frac{1}{b(\alpha^2-1)}[\tfrac{1}{2}\sinh(2bu)-\alpha\sinh(bu)]\ . \tag{3.5}$$

We introduce the new variables $y=2bu$, $t=T\Omega_0$, $X=x\Omega_0$ to rewrite (3.4) in the form

$$\partial_t^2 y-\partial_X^2 y+\frac{1}{\alpha^2-1}\left[\sinh(y)-2\alpha\sinh\left[\frac{y}{2}\right]\right]\ , \tag{3.6}$$

which is the double-sinh-Gordon equation. Its kink-antikink solutions can be obtained directly as

$$y=4\,\mathrm{arctanh}\left\{\pm\left[\frac{\alpha-1}{\alpha+1}\right]^{1/2}\tanh\left[\frac{X-st}{2(1-s^2)^{1/2}}\right]\right\}\ . \tag{3.7}$$

Here, s is the velocity ($s<s_0$ means subsonic whereas $s>s_0$ means supersonic velocities; note $s_0<1$). From (3.7) we conclude that for $s<1$ subsonic and supersonic kink and antikink solutions are possible. The kink solution [$u(\pm\infty)=\pm q_0$, i.e., the upper sign in (3.7)] represents a negative ionic defect, while an antikink [$u(\pm\infty)=\mp q_0$, i.e., the lower sign in (3.7)] represents a positive ionic defect. These exact solutions of the one-component model will now be generalized for the two-component description of this paper.

For two-component solitary waves, two cases are of interest: (1) $\Omega_i=0$ (the chain is isolated from any environment) and (2) $\Omega_i\neq 0$ (the chain is subjected to influences of some regular environment with the lattice period l equal to the chain spacing). In any case, the proton component $u=u_k(\xi)$ of a resulting (stationary) solitary-wave solution is a kink (or antikink) satisfying the boundary conditions $u_k(\pm\infty)=\pm q_0$ (or $\mp q_0$). The profile of this component and the interval of admissible velocities for the two-component solitary wave crucially depend on the presence or absence of the external substrate potential for the heavy ions. If the hydrogen-bonded chain is isolated, i.e., $\Omega_i=0$, the set of Eqs. (3.1)–(3.3) can be treated analytically, whereas in the case $\Omega_i\neq 0$, the solitary-wave solutions of these equations can be found only numerically [11].

For $\Omega_i=0$, it is sufficient to consider Eq. (3.1) and one of Eqs. (3.2) or (3.3). After integration of Eq. (3.3) we obtain from Eq. (3.1)

$$(s^2-1)\frac{d^2u}{d\xi^2}+\left[(s^2-1)+\frac{1}{\mu}(s^2-s_0^2)\right]\frac{d\rho}{d\xi}$$
$$+\mu\Omega_0^2\frac{d}{d\xi}g(u,\rho)=0\ , \tag{3.8}$$

which can be trivially integrated again. Therefore, the set of Eqs. (3.3) and (3.4) can be rewritten in the form of the dynamical equations

$$\frac{du}{d\xi}=(1-s^2)^{-1}\frac{\partial}{\partial\rho}\Phi(u,\rho)\ ,\quad \frac{d\rho}{d\xi}=(s^2-s_0^2)^{-1}\frac{\partial}{\partial u}\Phi(u,\rho) \tag{3.9}$$

on the plane (u,ρ) with "time" ξ, $-\infty<\xi<\infty$. The two-dimensional potential Φ is defined as

$$\Phi(u,\rho)=\frac{1}{2}\left[\left[1+\frac{1}{\mu}\right]s^2-\left[1+\frac{s_0^2}{\mu}\right]\right]\rho^2$$
$$+\mu\Omega_0^2[\tilde{U}(u,\rho)-g_0\rho]\ , \tag{3.10}$$

where $g_0=g(\pm q_0,0)$. Eliminating the variable ξ, we obtain

$$\frac{d\rho}{du}=\frac{1-s^2}{s^2-s_0^2}\left[\frac{\partial\Phi}{\partial u}\right]\Big/\left[\frac{\partial\Phi}{\partial\rho}\right]\ , \tag{3.11}$$

which can be analyzed qualitatively. For instance, one of the conditions which immediately follows from this equation is the existence of a gap that is near the velocity $s=s_0$ in the velocity spectrum $0\le s<1$.

Now we shall consider two additional (to $\Omega_i=0$) limiting cases when the gap in the velocity spectrum can be calculated explicitly [11]. In the *first* approximation, one assumes that the on-site potential

$$\tilde{U}=(\alpha^2/D_0)\{1/[2b^2(\alpha^2-1)]\}U$$

does not depend on the relative displacements ρ, i.e., the function $\tilde{U}=\tilde{U}(u)$ keeps its profile while moving with the heavy ions. In this particular case, the integration of Eqs. (3.9) and (3.11) gives

$$\frac{du_k}{d\xi}=\pm\gamma_1\Omega_0[2\tilde{U}(u_k)]^{1/2} \tag{3.12}$$

and

$$\rho_k=\mp\mu\Omega_0[2\tilde{U}(u_k)]^{1/2}/\gamma_1(s_0^2-s^2)\ , \tag{3.13}$$

where

$$\gamma_1=\left[\frac{1}{1-s^2}+\frac{\mu}{s_0^2-s^2}\right]^{1/2} \tag{3.14}$$

is the generalization of the "relativistic" factor $\gamma=(1-s^2)^{-1/2}$ in the (one-component) Frenkel-Kontorova (FK) model [16,17], when the heavy ions are frozen. Formally, the one-component limit can be obtained from (3.12)–(3.14) for $\mu=0$. The appearance of a gap in the solitary-wave velocity spectrum follows from (3.14). It appears for $s_0<s<s_1$, where

$$s_1=\left[\frac{s_0^2+\mu}{1+\mu}\right]^{1/2}, \quad s_0<s_1<1 . \tag{3.15}$$

The kink solution [for the upper signs in (3.8) and (3.9)] corresponds to the negative ionic defect, while the antikink (for the lower signs) describes the positive ionic defect.

Equation (3.12) for $u_k(\xi)$ has the same form as in the FK model. It can be integrated giving the well-known implicit kink solution for any on-site potential $\tilde{U}(u)$. Then the second component can be immediately calculated according to the relation (3.13) from which we can generally conclude that the positive defect (antikink) is accompanied by a localized rarefaction ($\rho_k>0$) if $0\le s<s_0$, or compression ($\rho_k<0$) if $s_1\le s<1$, while the negative defect (kink) is accompanied by a localized compression for $0\le s<s_0$, or rarefaction for $s_1<s<1$.

In the continuum limit the energy of a positive or negative ionic defect moving with velocity s can be calculated directly from the Hamiltonian (1.1). Using (1.4), (1.6), and (3.12)–(3.14), we obtain

$$E_1=\left[\frac{2^{1/2}}{\gamma_1}\right]^3\Omega_0 mc_0^2\left[\frac{1}{(1-s^2)^2}+\frac{\mu s_0^2}{(s_0^2-s^2)^2}\right]\times\int_0^{q_0}\tilde{U}(u)^{1/2}du . \tag{3.16}$$

It follows from this expression that, at the edges of the solitary-wave velocity spectrum, $E_1\to\infty$.

The *second* approximation (note that we are still in the $\Omega_i=0$ case) is opposite to the previous one. Here we keep the dependence of the on-site potential $\tilde{U}$ on ρ but neglect the effects due to the motion of the mass centers R_n. In other words, we assume in the Hamiltonian (1.1) that $q_n\approx u_n$ [see Eq. (1.4)] and set

$$\tilde{U}(q_n,Q_n,Q_{n+1})=\tilde{U}(u_n,\rho_n) .$$

Then we get the following pair of difference-differential equations:

$$\frac{d^2u_n}{dT^2}=u_{n+1}-2u_n+u_{n-1}-\Omega_0^2\tilde{f}_n , \tag{3.17}$$

$$\frac{d^2\rho_n}{dT^2}=s_0^2(\rho_{n+1}-2\rho_n+\rho_{n-1})+\mu\Omega_0^2(\tilde{g}_{n+1}-2\tilde{g}_n+\tilde{g}_{n-1}) , \tag{3.18}$$

which in the continuum limit take the form

$$u_{TT}-u_{xx}+\Omega_0^2\tilde{f}=0 , \tag{3.19}$$

$$\rho_{TT}-s_0^2\rho_{xx}=\mu\Omega_0^2\tilde{g}_{xx} . \tag{3.20}$$

For the waves of a stationary profile, Eq. (3.20) is easily integrated and we obtain

$$\rho=\mu\Omega_0^2(s^2-s_0^2)^{-1}[\tilde{g}(u,\rho)-\tilde{g}_0] . \tag{3.21}$$

In order to solve Eq. (3.21), we should perform some additional simplifications—namely, restrict ourselves to only the linear dependence on ρ in the on-site potential

$$\tilde{U}(u,\rho)=\tilde{U}(u)+\rho W(u)+O(\rho^2) , \tag{3.22}$$

where $\tilde{U}(u)=\tilde{U}(u,0)$ and $W(u)=\tilde{g}(u,0)$. Substituting (3.22) into Eqs. (3.19) and (3.20), we arrive at the model proposed in [8] and being studied afterwards for different particular cases [9].

Since the function (3.22) is linear in ρ, the derivative $\tilde{g}$ does not depend on this variable, i.e., $\tilde{g}=W(u)$, and therefore [see Eq. (3.21)]

$$\rho_k=\mu\Omega_0^2[W(u_k)-W_0]/(s^2-s_0^2) \tag{3.23}$$

and

$$\frac{du_k}{d\xi}=\pm\Omega_0\left[\frac{2U_e(u_k;s)}{1-s^2}\right]^{1/2}, \tag{3.24}$$

where $W_0=W(\pm q_0)$ and

$$U_e=\tilde{U}+\frac{\mu\Omega_0^2}{s^2-s_0^2}W\left[\frac{W}{2}-W_0\right] \tag{3.25}$$

is the effective potential depending on velocity s. Knowing the function $\tilde{U}(u,\rho)$, the potential U_e can be calculated explicitly. For example, for a double-quadratic potential we can write

$$\tilde{U}(u)=\tfrac{1}{2}(q_0-|u|)^2 \quad\text{and}\quad W(u)=(q_0-|u|) . \tag{3.26}$$

The last functions satisfy the simple relation $\tilde{U}(u)=2W^2(u)$ and therefore Eq. (3.24) can be simplified to the form (3.12) with γ_1 replaced by

$$\gamma_2=\left[\frac{1+\mu\Omega_0^2/4(s^2-s_0^2)}{1-s^2}\right]^{1/2}, \tag{3.27}$$

which becomes γ if $\mu=0$. Here we have again a gap, but now it is in the subsonic region, between the points

$$s_2=(s_0^2-\mu\Omega_0^2/4)^{1/2} \tag{3.28}$$

and s_0. As in the first limiting case, this gap also divides the velocity spectrum into two parts: slow (subsonic) and fast (supersonic) ones, but the behavior of the function γ_2 is different from that of the function $\gamma_1(s)$. Besides this, it follows from (3.23) that, contrary to the first approximation, both the kink and antikink are coupled with a localized compression (for $s<s_0$) or a localized rarefaction (for $s>s_0$) of the background sublattice.

The soliton energy (in the continuum approximation) can be also calculated [8] from the Hamiltonian (1.1) by using (3.23)–(3.25). The calculations are simplified if we generally put $W(u)=[\tilde{U}(u)/2]^{1/2}$ for all $-q_0<u<q_0$ as it takes place in the particular case (2.22). Then we obtain

$$E_2=\frac{2^{3/2}\Omega_0 mc_0^2}{(1-s^2)\gamma_2}\left[1+\mu\Omega_0^2\frac{2s-s_0^2-s^4}{4(s_0^2-s^2)^2}\right]\times\int_0^{q_0}\tilde{U}(u)^{1/2}du\ . \tag{3.29}$$

Both expressions, (3.16) and (3.29), have the well-known "relativistic" behavior in the limit $\mu\to 0$.

Furthermore, the kink widths in the vicinities of velocity values s_1 and s_2 tend to infinity. This means that the effective barrier for the proton transfer becomes very small and the proton kinks can move, even in those cases when they are pinned (immobile) in the framework of the usual FK model (where the heavy ions are assumed to be frozen). Then we can also conclude that at least near the velocity values s_1 and s_2, the continuum limit of the equations of motion was adopted correctly.

The numerical minimization scheme developed in [11] has confirmed the existence of a gap in the solitary-wave velocity spectrum for $\Omega_i=0$, but without any additional approximation. A numerical simulation of the full set of the basic equations of motion shows (for $\Omega_i=0$) that stable solitary-wave solutions exist in the region $0\le s<s_0$ and this is in agreement with the analytical results [8], while the solutions in the region $s_1<s<1$ are generally unstable (except for a small velocity band).

Now we turn to the second *case* $\Omega_i\neq 0$, where no exact solutions are known. For $\Omega_i\neq 0$ (e.g., $\Omega_i^2=0.1$, $s_0^2=0.1$), numerical simulations predict that there are no gaps in the velocity spectrum, but the allowed speed range is significantly reduced (e.g., to $0\le s\le 0.19$ for the parameters given above).

We conclude this subsection by a qualitative discussion of these phenomena. From Eq. (3.3) the forms of the solitons can be predicted. Let us assume that we have a kink or antikink solution for u with $u(\xi=0)=0$ and $u_{0\xi}\equiv u_\xi(\xi=0)>0$ (kink) or $u_\xi(\xi=0)<0$ (antikink) where $\xi=x-sT$. Furthermore, the solution for ρ should be bell shaped with $\rho_\xi(\xi=0)=0$, $\rho_0\equiv\rho(\xi=0)<0$, and $\rho_{0\xi\xi}\equiv\rho_{\xi\xi}(\xi=0)>0$ for compression, or $\rho(\xi=0)>0$ and $\rho_{\xi\xi}(\xi=0)<0$ for rarefaction, respectively. In the case of, e.g., two Morse potentials, the stationary form of Eq. (3.3) can then be written as

$$(s^2-s_0^2)\rho_{0\xi\xi}=-\Omega_i^2\rho_0+\Omega_0^2\mu\frac{u_{0\xi}}{(\alpha^2-1)}[e^{-b\rho_0}-\alpha e^{-b\rho_0/2}]\ . \tag{3.30}$$

From here the numerical results for $\Omega_i=0$ can be understood. If $|\rho_0|\ll 1$, the bracket [ ] on the right-hand side of (3.30) is negative and a kink ($u_{0\xi}>0$) can propagate supersonically ($s>s_0$) with rarefaction ($\rho_0>0$, $\rho_{0\xi\xi}<0$). Subsonic velocities ($s<s_0$) occur for a kink with compression ($\rho_0<0$, $\rho_{0\xi\xi}>0$). On the other hand, an antikink has just the opposite properties (for $\Omega_i=0$). Close to $s\approx s_0$, this consideration breaks down and a gap can occur. Obviously, going back to the dynamical equations, for $\Omega_i\neq 0$ the resonance of ρ is shifted from the resonance value $s^2=s_0^2$ (in the case $\Omega_i=0$).

B. Frequency-locked kink propagation

From other systems we know that besides stationary solitary-wave solutions, time-dependent stable solitary waves also exist. In this subsection we look for counterparts of the latter. Also, in contrast to Sec. III A, we fully take into account the discreteness effects. Thus, narrow solutions are also possible.

The numerical simulations of Sec. II B have shown that even for reasonable large amplitudes, periodic orbits exist (P1 single) for which, at the stroboscopic times, a proton is observed only in one potential well. The question is whether this stable single-particle motion can trigger a kink propagation. To answer this question, let us ignore (for the reason of simplicity) the motion of mass centers ($R_n=0$) and neglect the effects due to the inertia of the heavy ions ($\mu=0$), meaning that Eq. (1.9) is reduced to

$$\frac{d^2\rho_n}{dt^2}=\frac{v_0^2}{l^2}(\rho_{n+1}-2\rho_n+\rho_{n-1})-\omega_i^2\rho_n\ . \tag{3.31}$$

The solution of this equation will be inserted into Eq. (1.7) which, in the present approximation, reads

$$\frac{d^2u_n}{dt^2}=\frac{c_0^2}{l^2}(u_{n+1}-2u_n+u_{n-1})+\frac{1}{2}\frac{c_0^2}{l^2}(1-s_0^2)(\rho_{n+1}-\rho_{n-1})-\frac{1}{ml^2}f_n\ . \tag{3.32}$$

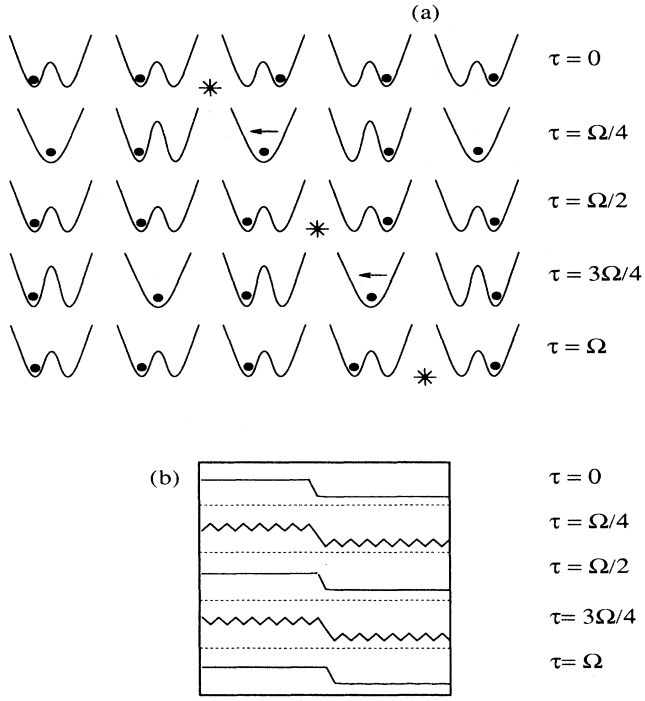

FIG. 6. Transportation mechanism by a kink, displayed during one period of the external driver: (a) Schematic plot of the proton positions in the time-varying potential well for five different times τ. The left arrow denotes the motion of the proton at the defect, whereas the asterisk designates the position of the defect. (b) Kink solutions $u_n(\tau)$ as a function of n for five different times τ.

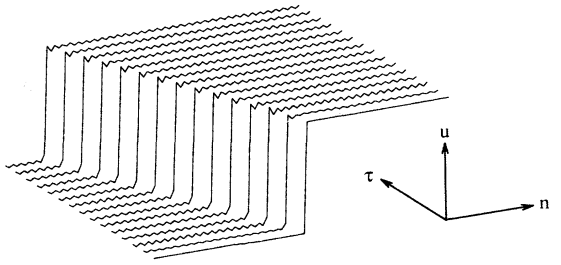

FIG. 7. Generation of a kink with small noise in the initial condition. The lower right distribution in n is for $\tau=0$; later times are shown progressively to the left.

Next, we introduce the nondimensional time τ [see Eq. (2.6)] and consider the optical mode

$$\rho_n(\tau)=(-1)^n\rho_0\sin(\Omega\tau) , \tag{3.33}$$

which is an exact solution of Eq. (3.31) for

$$\Omega^2=(4v_0^2/I^2\bar{\omega}^2)+\omega_i^2/\bar{\omega}^2 .$$

Inserting this into Eq. (3.32), we obtain [compare with Eqs. (2.7) or (2.9)]

$$\frac{d^2u_n}{d\tau^2}=\sigma_0^2(u_{n+1}-2u_n+u_{n-1}) - \frac{\partial}{\partial u_n}\bar{U}(u_n,\rho_n)-\gamma\frac{du_n}{d\tau} . \tag{3.34}$$

Here, as in Eq. (2.9), a phenomenological damping term γ has been introduced. Furthermore, $\sigma_0=c_0/l\bar{\omega}$, which can be considered as an adjustable parameter.

Before reporting the frequency-locked solution of the coupled equations (3.33) and (3.34), let us briefly mention the limiting case $\rho_0\equiv 0$. Then, in the case of two Morse potentials [see Eq. (3.5)], the kink solution located at site n_0 can be written as [compare with Eq. (3.7)]

$$u_n(\tau)=\frac{2}{b}\operatorname{arctanh}\left\{\pm\left[\frac{\alpha-1}{\alpha+1}\right]^{1/2} \times\tanh\left[\frac{1}{2}\left[\frac{\alpha+1}{\sigma_0^2-\sigma^2}\right]^{1/2} \times(n-n_0-\sigma\tau)\right]\right\} . \tag{3.35}$$

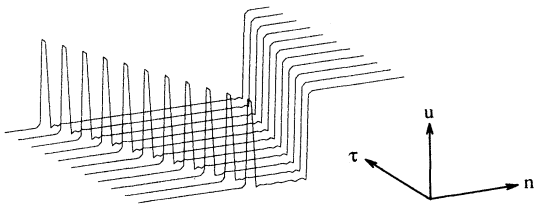

FIG. 8. Generation of a kink with larger noise in the initial condition, compared to that of Fig. 7.

We can take this form, for example, as an initial distribution for a solution of Eqs. (3.33) and (3.34) when $\rho_0\neq 0$.

We have solved Eqs. (3.33) and (3.34) numerically with standard leapfrog time stepping. The boundaries were assumed to be reflective. In Figs. 6–8 typically numerical results are shown for simulations with 100 protons and a small $\sigma_0=0.3$.

First, we present the most interesting result. Corresponding to the "P1 single" motion (above the threshold for the topology change of the potential $\bar{U}$) shown in Table I, there exists a frequency-locked kink propagation. The proton transport mechanism is the following: During half a period π/Ω of the frequency-locked period P1, a defect jumps from n_0 to n_0+1. Thus, within a *narrow* kink, a unique proton transport occurs. This mechanism is shown at the times 0, $\pi/2\Omega$, π/Ω, $3\pi/2\Omega$, and $2\pi/\Omega$ [from top to bottom in Figs. 6(a) and 6(b), respectively]. It means that the (anti)kink propagation velocity is determined by Ω in a unique manner. Numerical simulations show that this frequency-locked kink is quite stable. It also develops in time if we allow initially for noise, i.e., a quite random distribution of the protons in the right or left wells, respectively. A typical run is shown in Fig. 7. However, when the initial noise is too large, kink-antikink pairs can also be created, as shown in Fig. 8. But here, also, in the later stages of the time development, the velocities are determined by the frequency-locked proton motion.

IV. SUMMARY AND OUTLOOK

In this paper we have considered two aspects of the proton motion in hydrogen-bonded chains: first, the *individual* aspects leading to an oscillator model similar in form to the well-known Duffing oscillator. In this nonautonomous case, the external frequency appears in a natural way. Besides chaotic motion, we also found periodic motion (e.g., P1 single) in the large-amplitude case. This finding has consequences for the *collective* motion also: We can find propagating narrow kinks in the frequency-locked regime. These kinks seem to be attractors. They may be even more important than the wide kinks which were also discussed here. Note that the latter were obtained in the dissipationless case. Introduction of damping γ will eventually stop propagating (quasistationary) wide kinks and lead to a drastic reduction of their transport. Note that this latter negative effect does not occur for the frequency-locked kink propagation found here. Because of their importance for proton transport in hydrogen-bonded chains, the results for frequency-locked narrow kink propagation should be further considered in the future. Two generalizations are possible: First, the nonlinear dynamics should also be investigated from the Hamiltonian point of view, i.e., the coupling of the individual protons with the heavy ions is, more generally, a coupled nonlinear oscillator problem which could be also discussed within an autonomous conservative description. Secondly, the coupling of a kink with an external wave was here only considered in the short-wavelength limit of the optical mode. Finite k values and other modes may lead also to interesting results.

ACKNOWLEDGMENTS

One of the authors (A.V.Z.) is indebted to the University of Düsseldorf, where this work has been done, for its hospitality. This work has been supported by the European Community through Contract No. SC1-CT91-0705 and the Deutsche Forschungsgemeinschaft through SFB 237.

---

*Permanent address: Institute for Theoretial Physics, Ukrainian Academy of Sciences, 252130 Kiev, Ukraine.

[1] J. F. Nagle and S. Tristram-Nagle, J. Membrane Biology **74**, 1 (1983).

[2] J. H. Weiner and A. Askar, Nature **226**, 842 (1970).

[3] V. Ya. Antonchenko, A. S. Davydov, and A. V. Zolotaryuk, Phys. Status Solidi B **115**, 631 (1983).

[4] Y. Kashimori, T. Kikuchi, and K. Nishimoto, J. Chem. Phys. **77**, 1904 (1982).

[5] S. Yomosa, J. Phys. Soc. Jpn. **51**, 3318 (1982).

[6] E. W. Laedke, K. H. Spatschek, M. Wilkens, Jr., and A. V. Zolotaryuk, Phys. Rev. A **32**, 1161 (1985); M. Peyrard, S. Pnevmatikos, and N. Flytzanis, *ibid.* **36**, 903 (1987); H. Weberpals and K. H. Spatschek, *ibid.* **36**, 2946 (1987); H. Lan and K. Wang, *ibid.* **139**, 61 (1989).

[7] S. Yomosa, J. Phys. Soc. Jpn. **52**, 1866 (1983).

[8] A. V. Zolotaryuk, K. H. Spatschek, and E. W. Laedke, Phys. Lett. A **101**, 517 (1984).

[9] A. V. Zolotaryuk, Teor. Mat. Fiz. **68**, 415 (1986) [Sov. Theor. Math. Phys. **68**, 916 (1987)]; J. Halding and P. S. Lomdahl, Phys. Rev. A **37**, 2608 (1988); D. Hochstrasser, H. Büttner, H. Desfontaines, and M. Peyrard, *ibid.* **38**, 5332 (1988).

[10] A. V. Zolotaryuk and S. Pnevmatikos, in *Nonlinear World,* edited by A. G. Sitenko, V. E. Zakharov, and V. M. Chernousenko (Naukova Dumka, Kiev, 1989), Vol. 1, pp. 211–214.

[11] A. V. Zolotaryuk, S. Pnevmatikos, and A. V. Savin, Physica D **51**, 407 (1991).

[12] Y. Ueda, S. Yoshida, H. B. Stewart, and J. M. T. Thompson, National Institute for Fusion Science Report No. NIFS 20 (Nagoya, Japan, 1990) (unpublished).

[13] F. Varosi, C. Grebogi, and J. A. Yorke, Phys. Rev. Lett. A **124**, 59 (1987).

[14] C. S. Hsu, *Cell-to-Cell Mapping: A Method of Global Analysis for Nonlinear Systems* (Springer, New York, 1987).

[15] J. C. Fernandez, R. Grauer, K. Pinnov, and G. Reinisch, Phys. Rev. B **42**, 9987 (1990).

[16] J. Frenkel and T. Kontorova, J. Phys. (Moscow) **1**, 137 (1939).

[17] J. A. Krumhansl and J. R. Schrieffer, Phys. Rev. B **11**, 3535 (1975); J. F. Currie, J. A. Krumhansl, A. R. Bishop, and S. E. Trullinger, *ibid.* **22**, 477 (1980).